

ChemComm

Accepted Manuscript



This is an *Accepted Manuscript*, which has been through the Royal Society of Chemistry peer review process and has been accepted for publication.

Accepted Manuscripts are published online shortly after acceptance, before technical editing, formatting and proof reading. Using this free service, authors can make their results available to the community, in citable form, before we publish the edited article. We will replace this *Accepted Manuscript* with the edited and formatted *Advance Article* as soon as it is available.

You can find more information about *Accepted Manuscripts* in the [Information for Authors](#).

Please note that technical editing may introduce minor changes to the text and/or graphics, which may alter content. The journal's standard [Terms & Conditions](#) and the [Ethical guidelines](#) still apply. In no event shall the Royal Society of Chemistry be held responsible for any errors or omissions in this *Accepted Manuscript* or any consequences arising from the use of any information it contains.

COMMUNICATION

Linear assembly of porphyrin–C₆₀ complex confined in vertical nanocylinders of amphiphilic block copolymer films†

Cite this: DOI: 10.1039/x0xx00000x

Received 00th January 2014,
Accepted 00th January 2014

DOI: 10.1039/x0xx00000x

www.rsc.org/chemcomm

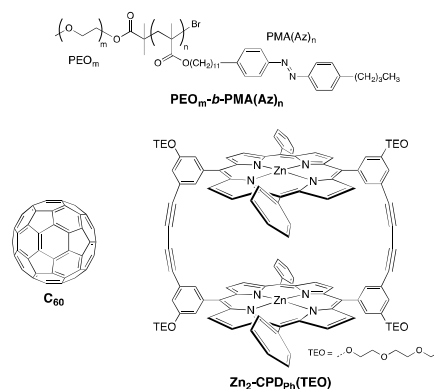
Takuya Kamimura,^a Motonori Komura,^{*b} Hideaki Komiyama,^c Tomokazu Iyoda^c and Fumito Tani^{*a}

Linear assemblies of 1:1 porphyrin–fullerene C₆₀ complex were formed in vertical cylindrical polyether nanodomains of amphiphilic block copolymer films by a simple spin coating–annealing method. The nanocylinder structures were kept even with high contents of the complex in the polymer films.

Porphyrin derivatives, which have a planar 18 π -electron system and strong absorption bands in UV to visible region, are generally good electron donors in their photoexcited states.^{1–3} Meanwhile, fullerenes, which have a spherical π -electron system, are excellent electron acceptors due to their favourable reduction potential and small reorganization energy in electron transfer reactions.^{4–7} Thus, supramolecular complexes composed of porphyrins and fullerenes have been extensively explored as artificial models for the charge separation in the reaction centre of photosynthesis and as promising materials applicable for organic photovoltaics (OPVs).⁸ From this viewpoint, we also have prepared cyclic porphyrin dimers (CPDs) that can include fullerene derivatives as guest molecules.^{9,10} The resulting inclusion complexes undergo photoinduced electron transfer from the porphyrins to the fullerenes to afford long-lived charge-separated states and photoelectric conversion.^{9c,d}

In order to realize high efficiency of photoelectric conversion, a well-ordered integration of a donor–acceptor (D–A) complex is required. Free charges derived from photoinduced charge separation of a D–A complex should be transported rapidly to an electrode without quenching by unfavourable charge recombination. Hence, a linear arrangement of a D–A complex is one of the ideal morphologies for smooth transportation of charges to an electrode. However, it has been rather difficult to control integration of a D–A complex by a rationally designable procedure, although there have recently been few examples for linear arrays of D–A complexes in photovoltaic systems.¹¹

One simple attractive method to build linear arrays of D–A complexes is to confine them into one-dimensional (1D) nanostructures of templates, such as vertical nanocylinders of organic (e.g. block copolymer)¹² and/or inorganic materials (e.g. aluminum oxide).¹³ This method has the following merits: (i) flexibility of molecular design of donors and acceptors is extended due to reduced need for self-organizing ability of molecules, (ii) size



Scheme 1. Chemical structures of PEO_m-b-PMA(Az)_n, C₆₀ and Zn₂-CPDPh(TEO).

of integrated arrays can be controlled readily by diameter and length of nanocylinders in applied templates. In this study, we have employed amphiphilic liquid crystalline block copolymers PEO_m-b-PMA(Az)_n (m and n mean degrees of polymerization of PEO and PMA, respectively) (Scheme 1) as template materials for confining the inclusion complex of CPD and C₆₀ in nanocylinders. PEO_m-b-PMA(Az)_n copolymers consist of hydrophilic poly(ethylene oxide) (PEO) and hydrophobic liquid crystalline poly(methacrylate) (PMA) with azobenzene (Az) mesogens in the side chains. PEO_m-b-PMA(Az)_n films formed on substrates have hexagonally-arranged vertical nanocylinders of PEO domains surrounded by PMA(Az) matrix.¹⁴ Diameter and interval of the cylindrical domains can be finely controlled by the degrees of polymerization of PEO and PMA, respectively. Moreover, the PEO cylindrical domains are in supercooled liquid phase at room temperature, which is suitable for introduction of molecules, metal nanoparticles and ions.^{15,16} We have recently shown that PEO_m-b-PMA(Az)_n copolymers function as templates for controlling arrangements of various molecules, metals, ions and polymers.¹⁷ Herein, we report formation of linear assemblies of a porphyrin–C₆₀ complex in cylindrical PEO domains of PEO_m-b-PMA(Az)_n films by a simple method (Scheme S1 in ESI).

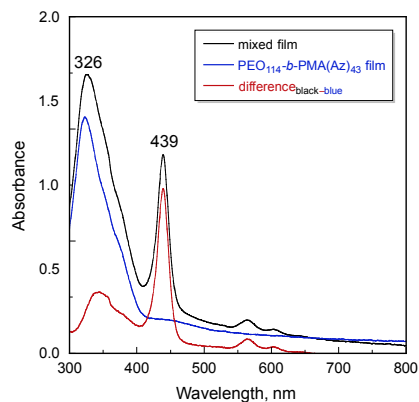


Figure 1. UV-vis absorption spectra of (black) mixed film of $C_{60} \square Zn_2$ -CPD_{Ph}(TEO) with PEO₁₁₄-*b*-PMA(Az)₄₃, (blue) PEO₁₁₄-*b*-PMA(Az)₄₃ film and (red) difference between the mixed film and PEO₁₁₄-*b*-PMA(Az)₄₃ film at room temperature. (black) content = 1/3. Thicknesses of the films were 100 nm.

Because porphyrin derivatives have generally poor solubility in hydrophilic solvents, we have designed and synthesized a new CPD modified with four triethylene oxide (TEO) chains on the *meso*-phenyl groups (Zn_2 -CPD_{Ph}(TEO), Scheme 1) to improve the solubility according to the reported procedure.^{9d} As a central metal of the porphyrin, zinc(II) ion was employed to determine the distribution of the inclusion complex composed of C_{60} and Zn_2 -CPD_{Ph}(TEO) ($C_{60} \square Zn_2$ -CPD_{Ph}(TEO)) in the mixed films with PEO_{*m*}-*b*-PMA(Az)_{*n*} by energy dispersive X-ray (EDX) spectroscopy. Zinc ion emits characteristic fluorescent X-ray which is not observed for light elements of C_{60} , Zn_2 -CPD_{Ph}(TEO) and PEO_{*m*}-*b*-PMA(Az)_{*n*}.¹⁸ Fluorescent X-ray of zinc detected in EDX images is expected to indicate the location of $C_{60} \square Zn_2$ -CPD_{Ph}(TEO) in the microphase-separated PEO_{*m*}-*b*-PMA(Az)_{*n*} films. Furthermore, zinc porphyrins are known to work as good electron donors in photoinduced electron transfer reactions.¹⁻³

The inclusion complex $C_{60} \square Zn_2$ -CPD_{Ph}(TEO) was prepared by mixing equal amount of C_{60} in a toluene solution and Zn_2 -CPD_{Ph}(TEO) in a $CHCl_3$ solution and then drying. The residual purple solid was readily dissolved in $CHCl_3$ as well as THF, both of which are poor solvents for C_{60} without inclusion by host compounds such as CPDs. On the basis of the photometric titration of Zn_2 -CPD_{Ph}(TEO) with C_{60} in toluene at 27 °C, the association constant (K_{assoc}) of $C_{60} \square Zn_2$ -CPD_{Ph}(TEO) was determined to be $6.0 \times 10^4 M^{-1}$ (Figure S1 in ESI).¹⁹ This high K_{assoc} value even in toluene, which is a good solvent for C_{60} , means that C_{60} is included by Zn_2 -CPD_{Ph}(TEO) in hydrophilic medium such as the PEO domains of PEO_{*m*}-*b*-PMA(Az)_{*n*}. UV-vis absorption spectrum of a thermally annealed mixed film of $C_{60} \square Zn_2$ -CPD_{Ph}(TEO) in PEO₁₁₄-*b*-PMA(Az)₄₃ (content = 1/3)²⁰ showed characteristic absorption bands at 326 and 439 nm (Figure 1), which are attributed to the π - π absorption of the liquid crystalline Az mesogen (Figure S2 in ESI) and the Soret band of $C_{60} \square Zn_2$ -CPD_{Ph}(TEO) (the blue line of Figure S1 in ESI), respectively. Based on the absorbance in the film and the extinction coefficient in solution of the Soret band, although the spectrum in the mixed film is slightly broaden, the number of moles per unit area (N_{mole}) of $C_{60} \square Zn_2$ -CPD_{Ph}(TEO) in the PEO₁₁₄-*b*-PMA(Az)₄₃ (content = 1/3) film is estimated to be 1×10^{-10} mole/cm².²¹ Similarly, the N_{mole} of the inclusion complex in the PEO₂₇₂-*b*-PMA(Az)₉₆ film (content = 1/2) is calculated to be 2×10^{-10} mole/cm².²¹ The mixed films of Zn_2 -CPD_{Ph}(TEO) in PEO₁₁₄-*b*-PMA(Az)₄₃ with various amounts of C_{60} were analyzed by UV-vis absorption spectroscopy (Figure S3 in ESI). The maximum wavelength (λ_{max}) of the Soret band of C_{60} -free Zn_2 -CPD_{Ph}(TEO) was 430 nm just after film preparation by spin coating. As the

amount of C_{60} increased, the Soret band was red-shifted to 440 nm and decreased in intensity with an isosbestic point at *ca.* 438 nm. Similar spectral changes were also observed for the mixed films after annealing as well as for the toluene solution. These results suggest that Zn_2 -CPD_{Ph}(TEO) in the PEO_{*m*}-*b*-PMA(Az)_{*n*} films surely includes C_{60} in the molecular cavity, as shown in the crystal structures of our previous inclusion complexes.^{9c}

Effects of the content of $C_{60} \square Zn_2$ -CPD_{Ph}(TEO) in PEO_{*m*}-*b*-PMA(Az)_{*n*} films coated on quartz plates were investigated by UV-vis absorption spectroscopy (Figure S4 in ESI). The λ_{max} of the Soret bands of the mixed films were *ca.* 440 nm before annealing irrespective of the content of the inclusion complex. However, after thermal annealing, the λ_{max} of the Soret bands showed contrasting changes dependent on the content. In the cases of the mixed films of the ratio below 1/3 for PEO₁₁₄-*b*-PMA(Az)₄₃ and 1/2 for PEO₂₇₂-*b*-PMA(Az)₉₆, the Soret bands slightly blue-shifted after annealing. On the other hand, in the cases of the mixed films with above these ratios, the Soret bands were faintly split and the red-shifted absorption peaks became larger than those of shorter wavelength. These results imply the followings: (i) under conditions of below the critical ratios, the inclusion complex is preferentially introduced into the PEO domains (*vide infra*), (ii) under conditions of above the critical ratios, the excess complex exists in a different environment such as the liquid crystalline PMA(Az) matrix to show the spectral changes.

The maximum contents of $C_{60} \square Zn_2$ -CPD_{Ph}(TEO) in PEO_{*m*}-*b*-PMA(Az)_{*n*} films for keeping the original nanocylinder structures were determined by atomic force microscopy (AFM) measurements. AFM phase images of thermal annealed films coated on quartz plates are shown in Figure 2. The well-ordered hexagonal alignment of the cylindrical PEO domains surrounded by PMA(Az) matrix was observed over a wide area for all mixed films. However, in the cases of the ratios above 1/3 for PEO₁₁₄-*b*-PMA(Az)₄₃ and 1/1.5 for PEO₂₇₂-*b*-PMA(Az)₉₆ (Figure 2b and 2d), some domains without cylindrical structure were observed. From these results, we determined the maximum contents to be 1/3 for PEO₁₁₄-*b*-PMA(Az)₄₃ and 1/1.5 for PEO₂₇₂-*b*-PMA(Az)₉₆. It is reasonable that

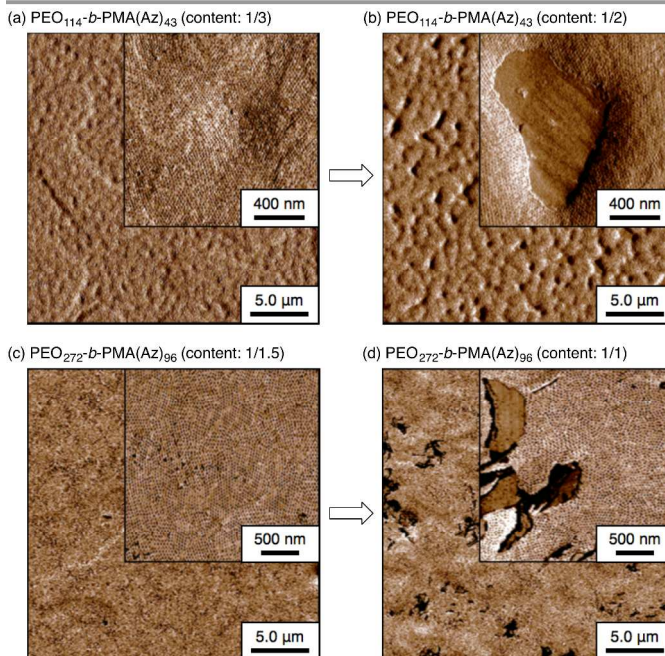


Figure 2. AFM phase images of the mixed films of $C_{60} \square Zn_2$ -CPD_{Ph}(TEO) with (a,b) PEO₁₁₄-*b*-PMA(Az)₄₃ and (c,d) PEO₂₇₂-*b*-PMA(Az)₉₆. The contents of $C_{60} \square Zn_2$ -CPD_{Ph}(TEO) and PEO_{*m*}-*b*-PMA(Az)_{*n*} are (a) 1/3, (b) 1/2, (c) 1/1.5 and (d) 1/1.

the longer PEO domain can accommodate relatively larger amount of the inclusion complex. On the basis of the AFM phase images, the average diameters of the cylindrical PEO domains were determined to be *ca.* 15 and 19 nm for the mixed films of PEO₁₁₄-*b*-PMA(Az)₄₃ and PEO₂₇₂-*b*-PMA(Az)₉₆, respectively.²² In addition, the AFM height profiles indicated that the average thicknesses of the mixed films were 100 nm for both block copolymers. The formation of the microphase-separated nanocylinder structure in the mixed films was also confirmed by grazing incidence small-angle X-ray scattering (GISAXS) measurements (Figure S5 in ESI).^{12c} The in-plane profiles showed two peaks with 1:√3 in *q*-scale indicating a hexagonally arranged structure of the nanocylinders. The average distances between two neighboring cylinders (*D*) were calculated to be 26 nm for PEO₁₁₄-*b*-PMA(Az)₄₃ and 40 nm for PEO₂₇₂-*b*-PMA(Az)₉₆ based on the *q* values. The numbers of cylindrical PEO domain per unit area (*N*_{cyl}) were determined to be 1.7×10^{11} for PEO₁₁₄-*b*-PMA(Az)₄₃ and 7.2×10^{10} cm⁻² for PEO₂₇₂-*b*-PMA(Az)₉₆.²³ Therefore, the amount of C₆₀□Zn₂-CPD_{Ph}(TEO) confined in one nanocylinder was calculated by using the above data. One nanocylinder of the mixed films of C₆₀□Zn₂-CPD_{Ph}(TEO) contains 6×10^{-22} mole (400 molecules) of the inclusion complex for PEO₁₁₄-*b*-PMA(Az)₄₃ film (content = 1/3, Figure 2a) and 3×10^{-21} mole (2000 molecules) for PEO₂₇₂-*b*-PMA(Az)₉₆ film (content = 1/2, Figure 2c). Further, on the basis of the average volumes of the nanocylinders, the pseudoconcentrations of the inclusion complex in the cylinder are considered to be 40 mM and 100 mM for PEO₁₁₄-*b*-PMA(Az)₄₃ film (content = 1/3) and PEO₂₇₂-*b*-PMA(Az)₉₆ film (content = 1/2), respectively. These concentrations are three orders higher than the reciprocal of the association constant ($1/K_{\text{assoc}} = 1.7 \times 10^{-5}$), assuring the inclusion of C₆₀ by Zn₂-CPD_{Ph}(TEO) in the mixed films.

The distribution of C₆₀□Zn₂-CPD_{Ph}(TEO) in the microphase-separated mixed films was analyzed by transmission electron microscopy (TEM) measurements. The hexagonally-arranged cylindrical structures were clearly observed in the TEM images of the RuO₄-stained mixed films of both PEO₁₁₄-*b*-PMA(Az)₄₃ and PEO₂₇₂-*b*-PMA(Az)₉₆ (Figure S6 in ESI). Moreover, it is notable that the microphase-separated structures were also confirmed in the images of the unstained mixed films (Figure S7 in ESI). These results indicate that heavy atoms exist in the cylindrical domains. In other words, the inclusion complex that contains zinc ion is introduced selectively into the cylindrical PEO domains in the microphase-separated mixed films. However, contrary to our expectation, signals of zinc ions were not detected by EDX spectroscopy for the PEO domains nor PMA(Az) matrix of the mixed films. On the other hand, zinc signals were clearly detected in all areas of the mixed films containing large excess of C₆₀□Zn₂-CPD_{Ph}(TEO) (Figure S8 in ESI). The absence of zinc signals for the mixed films of the appropriate content of C₆₀□Zn₂-CPD_{Ph}(TEO) would be due to the fact that the intensity of fluorescent X-ray of zinc was not enough for the EDX analysis.

We therefore applied thermal analysis as another method to confirm the selective introduction of C₆₀□Zn₂-CPD_{Ph}(TEO) into PEO domains in the microphase-separated mixed films. On cooling processes, both PEO₁₁₄-*b*-PMA(Az)₄₃ and PEO₂₇₂-*b*-PMA(Az)₉₆ have the following phase transitions: (i) from an isomeric phase (Iso) to a smectic A phase (SmA) of the PMA(Az) matrix at *ca.* 120 °C, (ii) from a smectic C phase (SmC) to an unknown smectic phase (SmX) of the PMA(Az) matrix at 80 °C, (iii) freezing transitions of the PEO domains at *ca.* 30 and -20 °C (Figure S9 in ESI).^{11a} We have carried out differential scanning calorimetry (DSC) analysis of the mixed films to investigate effects of the inclusion complex on these phase transitions. Obtained results are shown in Figure S10 and S11 in ESI. The transition temperatures of the PEO domains

decreased clearly as the increase of C₆₀□Zn₂-CPD_{Ph}(TEO). On the other hand, the Iso → SmA and SmC → SmX transition temperatures of the PMA(Az) matrix indicated only slight changes independent of the content. These contrastive results strongly suggest that the inclusion complex exists selectively in the cylindrical PEO domains of the mixed films rather than the PMA(Az) matrix.

In conclusion, we have demonstrated formation of linear assemblies of the inclusion complex of C₆₀ and oligoether-substituted cyclic porphyrin dimer in vertical cylindrical PEO domains in the microphase-separated PEO_{*m*}-*b*-PMA(Az)_{*n*} films by a simple method. The method consists of only spin coating of the mixed solution and thermal annealing. AFM, GISAXS and TEM measurements revealed that the inclusion complex can be incorporated into the PEO_{*m*}-*b*-PMA(Az)_{*n*} films with keeping the original nanocylinder structures under the conditions of within the appropriate contents, which were 1/3 for PEO₁₁₄-*b*-PMA(Az)₄₃ and 1/1.5 for PEO₂₇₂-*b*-PMA(Az)₉₆. In addition, TEM and DSC analysis confirmed the selective confinement of the inclusion complex in the cylindrical PEO domains in the mixed films. These successful results offer promise for the template method to build well-ordered one-dimensional arrays of organic photovoltaic materials.

This work was supported by Grants-in-Aid (No. 20108009 to F. T.) from Ministry of Education, Culture, Sports, Science and Technology of Japan, Research Grants from Nano-Macro Materials, Devices and System Research Alliance Project of our institutes and Research Grants to F.T. from Tokuyama Science and Technology Foundation and Iketani Science and Technology Foundation. We acknowledge Prof. K. Tamada of Kyushu University and Mr. H. Takami and Ms. S. Moriya of Asylum Technology Co. Ltd. for their kind cooperation on AFM measurements.

Notes and references

- ^a Institute for Materials Chemistry and Engineering, Kyushu University, 6-10-1 Hakozaki, Higashi-ku, Fukuoka, Fukuoka 812-8581, Japan. E-mail: tanif@ms.ifoc.kyushu-u.ac.jp; Fax: +81-92-642-2732; Tel: +81-92-642-2732
- ^b National Institute of Technology, Numazu College, 3600 Ooka Numazu, Shizuoka 410-8501, Japan. E-mail: m-komura@numazu-ct.ac.jp; Fax: +81-55-926-5704; Tel: +81-55-926-5704
- ^c Chemical Resources Laboratory, Tokyo Institute of Technology, 4259 Nagatsuta-cho, Midori-ku, Yokohama, Kanagawa 226-8503, Japan.
- † Electronic Supplementary Information (ESI) available: experimental details, synthesis and experimental data. See DOI: 10.1039/c000000x/

- 1 K. M. Kadish, K. M. Smith and R. Guilard, ed. *The Porphyrin Handbook*, Academic Press, San Diego, 2000.
- 2 K. M. Kadish, K. M. Smith and R. Guilard, ed. *Handbook of Porphyrin Science*, World Scientific, Singapore, 2010.
- 3 For reviews, see. (a) D. Gust, T. A. Moore and A. L. Moore, *Acc. Chem. Res.*, 2001, **34**, 40–48; (b) S. Fukuzumi, *Org. Biomol. Chem.*, 2003, **1**, 609–620; (c) M. E. El-Khouly, O. Ito, P. M. Smith and F. D'Souza, *J. Photochem. Photobiol. C: Photochemistry Reviews*, 2004, **5**, 79–104; (d) D. M. Guldi, G. M. A. Rahman, F. Zerbetto and M. Prato, *Acc. Chem. Res.*, 2005, **38**, 871–878; (e) S. Fukuzumi, *Phys. Chem. Chem. Phys.*, 2008, **10**, 2283–2297.
- 4 L. Echegoyen, F. Diederich and L. E. Echegoyen, in *Fullerenes: Chemistry, Physics and Technology*, ed. K. M. Kadish and R. S. Ruoff, Wiley-Interscience, New York, 2000, pp. 1–51.

- 5 S. Fukuzumi and D. M. Guldi, in *Electron Transfer in Chemistry*, ed. V. Balzani, Wiley-VCH, Weinheim, 2001, vol. 2, pp. 270–337.
- 6 D. M. Guldi and S. Fukuzumi, in *Fullerenes: From Synthesis to Optoelectronic Properties*, ed. D. M. Guldi and N. Martin, Kluwer, Dordrecht, 2003, pp. 237–265.
- 7 A. Hirsch and M. Brettreich, *Fullerenes: Chemistry and Reactions*, Wiley-VCH, Weinheim, 2005.
- 8 For reviews, see. (a) N. Martín, L. Sánchez, M. A. Herranz, B. Illescas and D. M. Guldi, *Acc. Chem. Res.*, 2007, **40**, 1015–1024; (b) S. Günes, H. Neugebauer and N. S. Sariciftci, *Chem. Rev.* 2007, **107**, 1324–1338; (c) P. V. Kamat, *J. Phys. Chem. C*, 2007, **111**, 2834–2860; (d) F. D'Souza and O. Ito, *Chem. Commun.* 2009, 4913–4928; (e) H. Imahori, T. Umeyama, K. Kurotobi and Y. Takano, *Chem. Commun.*, 2012, **48**, 4032–4045; (f) D. Gust, T. A. Moore and A. L. Moore, *Faraday Discuss.*, 2012, **155**, 9–26; (g) G. Bottari, O. Trukhina, M. Ince and T. Torres, *Coord. Chem. Rev.* 2012, **256**, 2453–2477; (h) D. I. Schuster, *J. Org. Chem.* 2013, **78**, 6811–6841; (i) S. Fukuzumi and K. Ohkubo, *Dalton Trans.* 2013, **42**, 15846–15858.
- 9 (a) H. Nobukuni, Y. Shimazaki, F. Tani and Y. Naruta, *Angew. Chem., Int. Ed.*, 2007, **46**, 8975–8978; (b) H. Nobukuni, F. Tani, Y. Shimazaki, Y. Naruta, K. Ohkubo, T. Nakanishi, T. Kojima, S. Fukuzumi and S. Seki, *J. Phys. Chem. C*, 2009, **113**, 19694–19699; (c) H. Nobukuni, Y. Shimazaki, H. Uno, Y. Naruta, K. Ohkubo, T. Kojima, S. Fukuzumi, S. Seki, H. Sakai, T. Hasobe and F. Tani, *Chem.–Eur. J.*, 2010, **16**, 11611–11623; (d) T. Kamimura, K. Ohkubo, Y. Kawashima, H. Nobukuni, Y. Naruta, F. Tani and S. Fukuzumi, *Chem. Sci.*, 2013, **4**, 1451–1461; (e) K. Sakaguchi, T. Kamimura, H. Uno, S. Mori, S. Ozako, H. Nobukuni, M. Ishida and F. Tani, *J. Org. Chem.*, 2014, **79**, 2980–2992.
- 10 For other typical reports of porphyrin–fullerene inclusion complexes: (a) P. D. W. Boyd and C. a Reed, *Acc. Chem. Res.*, 2005, **38**, 235–242; (b) K. Tashiro and T. Aida, *Chem. Soc. Rev.*, 2007, **36**, 189–197; (c) D. Canevet, E. M. Pérez and N. Martín, *Angew. Chem., Int. Ed.*, 2011, **50**, 9248–9259; (d) J. Zhang, X. Zheng, R. Jiang, Y. Yu, Y. Li, H. Liu, Q. Li, Z. Shuai and Y. Li, *RSC Adv.*, 2014, **4**, 27389–27392.
- 11 (a) A. Kira, T. Umeyama, Y. Matano, K. Yoshida, S. Isoda, J. K. Park, D. Kim and H. Imahori, *J. Am. Chem. Soc.*, 2009, **131**, 3198–3200; (b) Y. Matsuo, Y. Sato, T. Niinomi, I. Soga, H. Tanaka and E. Nakamura, *J. Am. Chem. Soc.*, 2009, **131**, 16048–16050; (c) K. Kanaizuka, A. Izumi, M. Ishizaki, H. Kon, T. Togashi, R. Miyake, T. Ishida, R. Tamura, M. Haga, Y. Moritani, M. Sakamoto and M. Kurihara, *ACS Appl. Mater. Interfaces*, 2013, **5**, 6879–6885; (d) Z. Wang, T. Miyadera, T. Yamanari and Y. Yoshida, *ACS Appl. Mater. Interfaces*, 2014, **6**, 6369–6377.
- 12 (a) T. Thurn-Albrecht, J. Schotter, G. A. Kästle, N. Emley, T. Shibauchi, L. Krusin-Elbaum, K. Guarini, C. T. Black, M. T. Tuominen and T. P. Russell, *Science*, 2000, **290**, 2126–2129; (b) Y.-C. Tseng and S. B. Darling, *Polymers*, 2010, **2**, 470–489; (c) J. K. Kim, S. Y. Yang, Y. Lee and Y. Kim, *Prog. Polym. Sci.*, 2010, **35**, 1325–1349; (d) Y. Deng, J. Wei, Z. Sun and D. Zhao, *Chem. Soc. Rev.*, 2012, 4054–4070; (e) Q. Jiang and M. D. Ward, *Chem. Soc. Rev.*, 2014, **43**, 2066–2079.
- 13 (a) F. Keller, M. S. Hunter and D. L. Robinson, *J. Electrochem. Soc.*, 1953, **100**, 411–419; (b) K. Itaya, S. Sugawara, K. Arai and S. Saito, *J. Chem. Eng. Jpn.*, 1984, **17**, 514–520; (c) F. Li, L. Zhang and R. M. Metzger, *Chem. Mater.*, 1998, **10**, 2470–2480.
- 14 (a) Y. Tian, K. Watanabe, X. Kong, J. Abe and T. Iyoda, *Macromolecules*, 2002, **35**, 3739–3747; (b) M. Komura and T. Iyoda, *Macromolecules*, 2007, **40**, 4106–4108; (c) M. Komura, K. Watanabe, T. Iyoda, T. Yamada, H. Yoshida and Y. Iwasaki, *Chem. Lett.*, 2009, **38**, 408–409; (d) S. Asaoka, T. Uekusa, H. Tokimori, M. Komura, T. Iyoda, T. Yamada and H. Yoshida, *Macromolecules*, 2011, **44**, 7645–7658.
- 15 (a) S. Watanabe, R. Fujiwara, M. Hada, Y. Okazaki and T. Iyoda, *Angew. Chem., Int. Ed.*, 2007, **46**, 1120–1123; (b) T. Yamamoto, T. Kimura, M. Komura, Y. Suzuki, T. Iyoda, S. Asaoka and H. Nakanishi, *Adv. Funct. Mater.*, 2011, **21**, 918–926.
- 16 It has been confirmed that the nanocylinders of PEO_m-b-PMA(Az)_n have ability to accommodate fairly large amount of exogenous substances with keeping the hexagonal arrangements. For detailed reports of their morphologies: (a) R. Watanabe, K. Kamata and T. Iyoda, *J. Mater. Chem.*, 2008, **18**, 5482–5491; (b) H. Komiyama, R. Sakai, S. Hadano, S. Asaoka, K. Kamata, T. Iyoda, M. Komura, T. Yamada and H. Yoshida, *Macromolecules*, 2014, **47**, 1777–1782.
- 17 (a) J. Li, K. Kamata, S. Watanabe and T. Iyoda, *Adv. Mater.*, 2007, **19**, 1267–1271; (b) A. Chen, M. Komura, K. Kamata and T. Iyoda, *Adv. Mater.*, 2008, **20**, 763–767; (c) J. Li, K. Kamata and T. Iyoda, *Thin Solid Films*, 2008, **516**, 2577–2581; (d) J. Z. Li, Y. Wang, Z. Hong Wang, D. Mei, W. Zou, A. Min Chang, Q. Wang, M. Komura, K. Ito and T. Iyoda, *Ultramicroscopy*, 2010, **110**, 1338–1342; (e) T. Goda and T. Iyoda, *J. Mater. Chem.*, 2012, **22**, 9477–9480; (f) B. X. Dong, Y. Honmou, H. Komiyama, S. Furumaki, T. Iyoda and M. Vacha, *Macromol. Rapid Commun.*, 2013, **34**, 492–497.
- 18 A. J. Markowicz, in *Handbook of X-Ray Spectrometry, Second Edition, Revised and Expanded*, ed. R. E. van Grieken and A. J. Markowicz, Marcel Dekker, 2002, pp. 47–52.
- 19 The K_{assoc} was determined by the following equation by applying a non-linear curve-fitting method to changes in absorbance upon the titration of Zn₂-CPD_{Ph}(TEO) (monitored at 424 nm) with C₆₀:
- $$\Delta Abs = L \times \frac{1 + K_{\text{assoc}} A + K_{\text{assoc}} X - \sqrt{(1 + K_{\text{assoc}} A + K_{\text{assoc}} X)^2 - 4 K_{\text{assoc}} A X}}{2 K_{\text{assoc}} A}$$
- where A and X are [Host]₀ and [Guest]₀, respectively; L is ΔAbs at 100 % complexation; L and K_{assoc} are treated as fitting parameters.
- 20 The content of C₆₀–Zn₂-CPD_{Ph}(TEO) in the polymer films is expressed as the mixing weight ratio of the inclusion complex to the PEO domains *i.e.* {C₆₀–Zn₂-CPD_{Ph}(TEO)}/{PEO block in PEO_m-b-PMA(Az)_n} (w/w).
- 21 The number of moles per unit area of C₆₀–Zn₂-CPD_{Ph}(TEO) in the mixed film (N_{m} , mole/cm²) is estimated by the following equation:
- $$N_{\text{mole}} = Abs_{\text{film}} / (\varepsilon \times 10^3)$$
- where Abs_{film} is maximum absorbance of the Soret band of the mixed film; ε of C₆₀–Zn₂-CPD_{Ph}(TEO) in solution is *ca.* $5 \times 10^5 \text{ cm}^{-1} \text{ M}^{-1}$.
- 22 These diameters are very close to the reported values of the pure PEO_m-b-PMA(Az)_n films within experimental errors; 14 nm for PEO₁₁₄-b-PMA(Az)₄₃ and 22 nm for PEO₂₇₂-b-PMA(Az)₉₆. (a) M. Komura, H. Komiyama, K. Nagai and T. Iyoda, *Macromolecules*, 2013, **46**, 9013–9020 and reference 17a.
- 23 The number of the nanocylinder per unit area in the film (N_{cyl} , cm⁻²) is estimated by the following equation:
- $$N_{\text{cyl}} = 2 \times 10^{14} / (\sqrt{3} \times D^2)$$

where D (nm) is the average distance between two neighbouring cylinders.